

**Ni(II) Complexes of the Phosphine-Oxime Ph₂PC₆H₄-2-CH=NOH**

Journal:	<i>Dalton Transactions</i>
Manuscript ID	DT-ART-04-2018-001551.R1
Article Type:	Paper
Date Submitted by the Author:	04-May-2018
Complete List of Authors:	Basu, Debashis; University of Illinois at Urbana-Champaign, School of Chemical Sciences Woods, Toby; University of Illinois at Urbana-Champaign, School of Chemical Sciences Rauchfuss, Thomas; University of Illinois at Urbana-Champaign, School of Chemical Sciences

Ni(II) Complexes of the Phosphine-Oxime Ph₂PC₆H₄-2-CH=NOH

Debashis Basu, Toby J. Woods, Thomas B. Rauchfuss*

School of Chemical Sciences

University of Illinois

Urbana, IL 61801, USA

Abstract

We report the solution and structural chemistry of a nickel(II) complexes of the phosphine-oxime Ph₂PC₆H₄-2-CH=NOH (PCH=NOH). PCH=NOH invariably binds in a bidentate manner, both as the neutral ligand and as its conjugate base as illustrated by *cis*-Ni(PCH=NOH)₂Cl₂ and diamagnetic *cis*-[Ni(PCH=NOH)₂]²⁺ (as its BF₄⁻ salt). Treatment of PCH=NOH with Ni(OAc)₂(H₂O)₄ gave charge-neutral *trans*-[Ni(PCH=NO)₂]⁰. Treatment of *trans*-[Ni(PCH=NO)₂]⁰ with BF₃ gave [Ni(PCH=NO)₂BF₂]⁺BF₄⁻. The cation features a planar NiP₂N₂ center wherein the pair of oximate groups are linked by the difluoroboryl center. The 1:1 complexes of the oxime and the oximate are illustrated by [Ni(PCH=NOH)Cl₂]₂ and [Ni(C₆F₅)(PCH=NO)]₂, which feature five- and four-coordinate Ni(II) centers, respectively. All complexes in this series hydrolyze to give the trinickel oxo-phosphine-oximate complex [Ni₃(PCH=NO)₃O]⁺. One feature of the PCH=NOH ligand is its wide bite angle combined with its protic OH center. These aspects are manifested in the structures of Ni(PCH=NOH)₂Cl₂ and [Ni(PCH=NOH)Cl₂]₂, which show intramolecular hydrogen bonding to terminal chloride ligands.

Introduction

Nickel complexes of P-N ligands are represented by derivatives of phosphine-imines,¹ phosphine-oxazolines,² phosphine-pyrazoles,³ and phosphine-diazaene.⁴ Example of nickel complexes of phosphine-oximes are unknown despite the powerful precedent of nickel(II) bis(dimethylglyoximate) and the fact that oximates form multimetallic frameworks.⁵ Both Ni-oxime⁶ and Ni-phosphine⁷ complexes are well developed, which spurred our interest in the behavior of the phosphine-oxime $\text{Ph}_2\text{PC}_6\text{H}_4\text{CH}=\text{NOH}$, abbreviated $\text{PCH}=\text{NOH}$. Illustrative complexes of $\text{PCH}=\text{NOH}$ and a related ligand are presented in In Figure 1.⁸

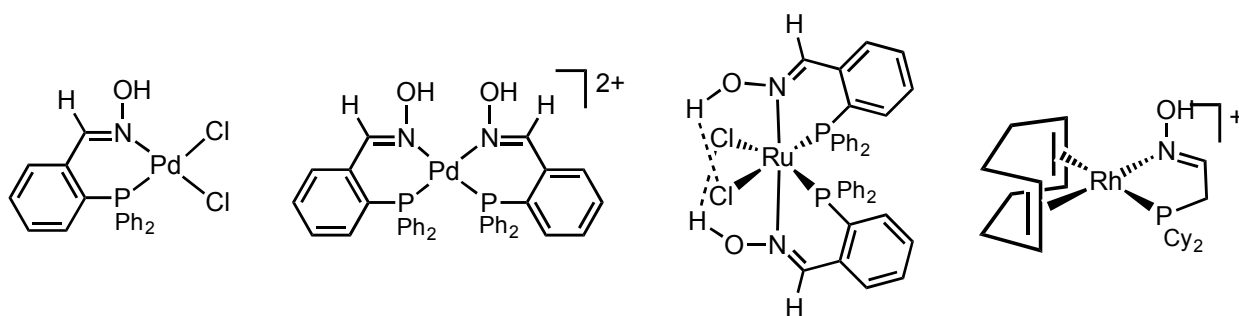
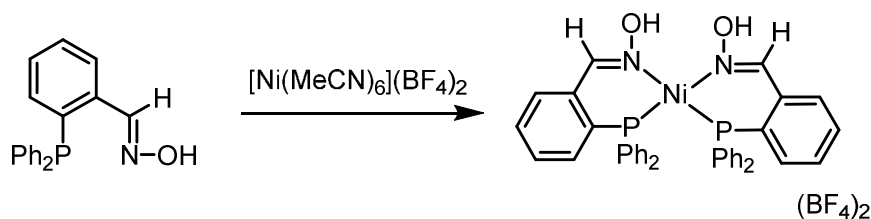


Figure 1. Illustrative phosphine-oxime complexes.

Results and Discussion

2:1 Complexes $[\text{Ni}(\text{PNOH})_2]^{2+}$ and $\text{Ni}(\text{PNO})_2$. The parent complexes in this study are $[\text{Ni}(\text{PCH}=\text{NOH})_2]^{2+}$ and its conjugate base $\text{Ni}(\text{PNO})_2$. The former was obtained from reaction of $\text{PCH}=\text{NOH}$ and $[\text{Ni}(\text{MeCN})_6](\text{BF}_4)_2$ (Scheme 1).



Scheme 1. Synthesis of $[\text{cis-Ni}(\text{PCH}=\text{NOH})_2](\text{BF}_4)_2$ ($[\mathbf{1H}_2](\text{BF}_4)_2$).

The resulting orange-colored salt $[\text{Ni}(\text{PCH}=\text{NOH})_2](\text{BF}_4)_2$ ($[\mathbf{1H}_2](\text{BF}_4)_2$) proved to be very labile but was eventually obtained as single crystals. According to X-ray crystallography (Figure 2), the dication $[\mathbf{1H}_2]^{2+}$ is cis-square planar with Ni-N (~ 1.96 Å) and Ni-P (~ 2.2 Å) bond distances consistent with low-spin Ni(II). ^{31}P NMR spectroscopy corroborates the diamagnetism of this complex (Figure S1). Weak hydrogen bonding is evident between oxime O-H and BF_4^- counterions (Figure 2).

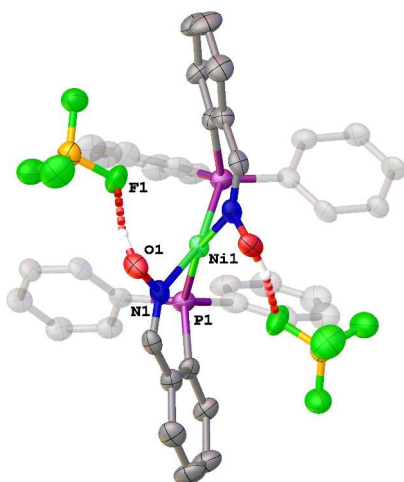
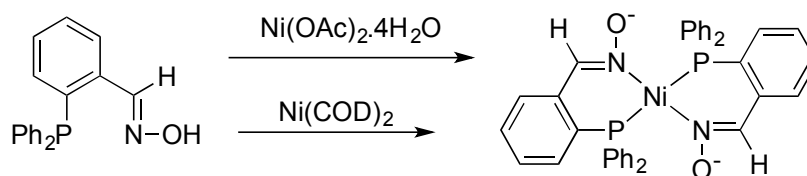


Figure 2. Thermal ellipsoid plot (50 % probability) of *cis*- $[\text{Ni}(\text{PCH}=\text{NOH})_2]^{2+}$ ($[\mathbf{1H}_2]^{2+}$). Most hydrogen atoms were removed for clarity. The oxime phenyl ring atoms have been faded for clarity. Unlabeled hetero atoms are related by the symmetry operator (1-x, 1-y, +z). The O-H \cdots F interaction is denoted by the dashed red line.

The two P-N chelates are not coplanar as indicated by the dihedral angle of $25.24(19)^\circ$ between the $\text{NiP}(1)\text{N}(1)$ and $\text{NiP}(1')\text{N}(1')$ planes. Consequently, the two hydroxyl oxygen centers are widely separated ($2.992(8)$ Å).

The conjugate base of $[\mathbf{1H}_2]^{2+}$ is $[\mathbf{1}]^0$, which was obtained by combining PCH=NOH with half an equivalent of $\text{Ni}(\text{OAc})_2 \cdot 4\text{H}_2\text{O}$. The product is the red-orange diamagnetic complex $\text{Ni}(\text{PCH}=\text{NO})_2$ ($\mathbf{1}$). The same complex arises from the reaction of

PCH=NOH and Ni(COD)₂ (COD = 1,5-cyclooctadiene). Precedent suggests that this reaction could proceed with concomitant release of H₂ or cyclooctene (Scheme 2).⁹



Scheme 2. Syntheses of *trans*-Ni(PCH=NO)₂ ([1]⁰).

X-ray crystallographic analysis of [1]⁰ established the *trans* geometry (Figure 3). It is structurally similar to bis(phosphine-pyrazolate) complexes of Ni(II).³ The Ni(II) center is square planar ($\tau_4' = 0.2886$), with a planarity deviation of 0.75 (RMSD/Å). The Ni-ligand bond-lengths confirm the low-spin character of this d⁸-Ni^{II} complex, consistent with well resolved NMR spectra (Figure S2).

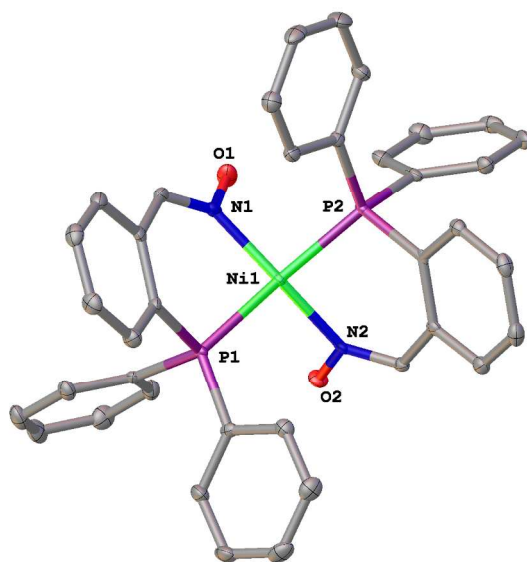
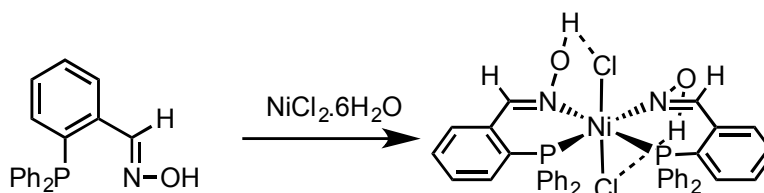


Figure 3. Thermal ellipsoid plot (50 % probability) of *trans*-Ni(PCH=NO)₂ ([1]⁰). Most hydrogen atoms were removed for clarity. Selected bond distances (Å): Ni-N3: 1.86, Ni-N4: 1.87, Ni-P3: 2.19, Ni-P4: 2.20.

A third member of this series of 2:1 complexes has the formula $\text{Ni}(\text{PCH}=\text{NOH})_2\text{Cl}_2$. Abbreviated [$\mathbf{1H}_2\text{Cl}_2$], this robust complex was obtained by combining $\text{PCH}=\text{NOH}$ and $\text{NiCl}_2 \cdot 6\text{H}_2\text{O}$ in $\text{CH}_2\text{Cl}_2/\text{MeOH}$ solution (Scheme 3).



Scheme 3. Synthesis of $\text{Ni}(\text{PCH}=\text{NOH})\text{Cl}_2$, $\mathbf{1H}_2\text{Cl}_2$.

It crystallizes easily as green prisms. X-ray crystallographic analysis confirmed that [$\mathbf{1H}_2\text{Cl}_2$] is pseudo-octahedral (Figure 4). The long Ni-L bond distances (Ni-N (~ 2.1 Å), Ni-P (~ 2.4 Å), and Ni-Cl (~ 2.4 Å)) reaffirm the high-spin nature of the complex. The two chloride ligands are mutually trans. These axial chloride ligands form hydrogen bonds with the oxime as indicated by the short O-H \cdots Cl distances of ~ 2.3 Å. Given that the Ni-Cl bonding is more ionic in high spin Ni(II), such hydrogen bonding is stabilized by the anionic nature of the chloride ligand. The magnetic moment of the complex is 2.39 B.M., consistent with a triplet ground state (Figure S3). Other $\text{NiCl}_2(\text{P-N})_2$ complexes

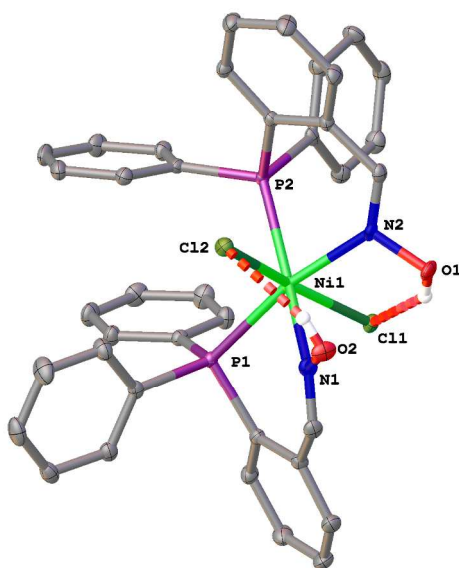
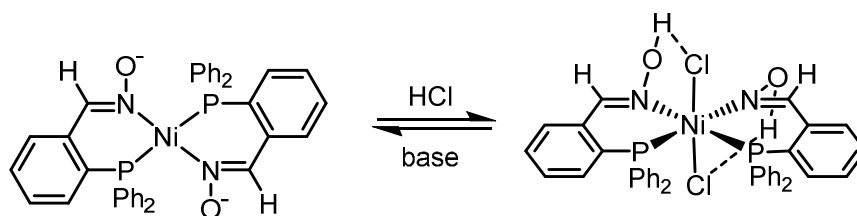


Figure 4. Thermal ellipsoid plot (50 % probability) of *cis*- $\text{Ni}(\text{PCH}=\text{NOH})\text{Cl}_2$, $\mathbf{1H}_2\text{Cl}_2$. Most H atoms were removed for clarity. The O-H \cdots Cl interaction is denoted by the red dashes.

have been reported where P-N is a phosphine-oxazoline/pyridine.¹⁰

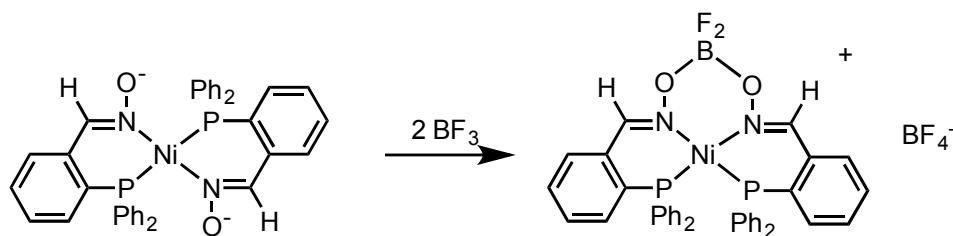
[Ni(PCH=NOH)₂]²⁺ as a Lewis and Bronsted Acid. Deprotonation of [1H₂Cl₂] gave [1]⁰, illustrating the coupling of acid-base behavior and a change in magnetism. Thus, addition of slight excess of Et₃N to a methanol solution of [1H₂Cl₂] generated [1]⁰, as signaled by a color change of green to orange (Scheme 4). The reverse reaction, protonation of [1]⁰, is complicated by the lability of [1H₂]²⁺. As a dication with two H-bonding donors (oxime groups), [1H₂]²⁺ is a Lewis acid with an affinity for chloride. This property was indicated by the reaction of [1]⁰ with two equiv of HCl to generate [1H₂Cl₂] (Scheme 4). The relationship of low-spin [1]⁰ and hydrogen-bonded high-spin [1H₂Cl₂] has precedent. Nickel bis(dimethylglyoximate) is famously low-spin, in contrast to octahedral *cis*-dichloronickel bis(dimethylglyoxime),¹¹ which features hydrogen bonds between chloride and the hydroxyl groups.



Scheme 4. Interconversion of complex **1** and **1H₂Cl₂**.

BF₂-Capped Complex. An iconic reaction of Ni(dmgh)₂ is its capping reaction with BF₃ to give Ni(dmghBF₂)₂. An analogous process was observed upon treatment of *trans*-[Ni(PCH=NO)₂]⁰ with BF₃, which serves as a source of both BF₂⁺ and BF₄⁻. The product is the pale-yellow salt [Ni(PCH=NO)₂BF₂]⁺BF₄⁻ wherein the pair of oximate groups are linked by the difluoroboryl center. The conversion implies rapid isomerization of either *trans*-[Ni(PCH=NO)₂] or an adducts such as *trans*-[Ni(PCH=NOBF₃)₂]. The salt

$[\text{Ni}(\text{PCH}=\text{NO})_2\text{BF}_2]\text{BF}_4$ was initially characterized by its ^{19}F NMR spectrum, which shows two signals in an intensity ratio of 2:1 assigned to the BF_4 and BF_2 centers, respectively (Figure S4). ESI-MS and ^{31}P NMR spectra further support the proposed formulation (Figure S5, S6, Scheme 5). Cyclic voltammetry of $[\text{Ni}(\text{PCH}=\text{NO})_2\text{BF}_2]\text{BF}_4$ reveals a quasi-reversible 1e reduction at -0.78 V vs $\text{Fc}^{+/0}$ (Figure S7), which is 190 mV milder than the reduction reported for a related cationic Ni(II) diimine-dioximate.^{6a}



Scheme 5. BF_2 -Capping reaction of **1**.

According to X-ray crystallography (Figure 5), the coordination geometry of the Ni center of the monocation $[\mathbf{1}\text{BF}_2]^+$ is almost square planar. The dihedral angle between P2-Ni1-N2 and P1-Ni1-N1 planes is $5.02(6)^\circ$. The Ni-N (~ 1.95 Å) and Ni-P (~ 2.2 Å) bond distances are consistent with low-spin Ni(II). The boron center is tetrahedral.

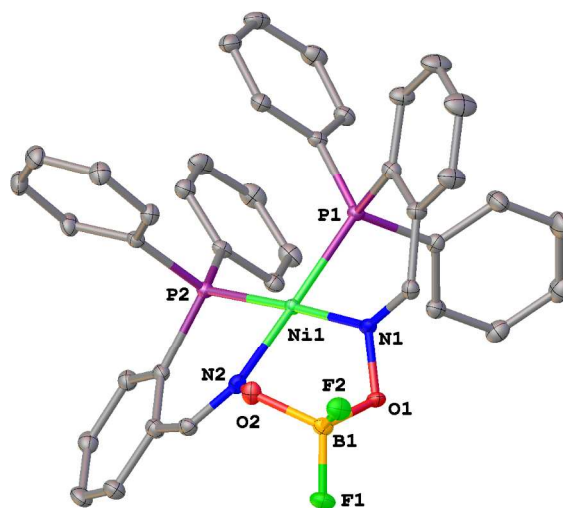
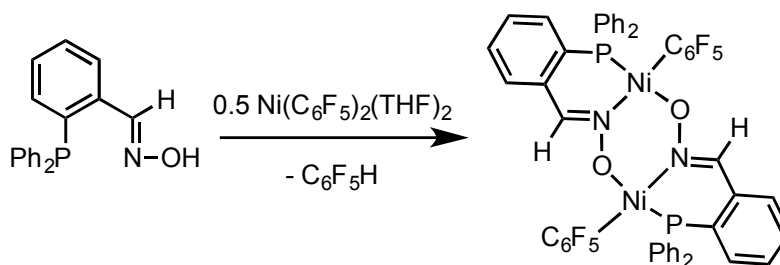


Figure 5. Thermal ellipsoid plot (50 % probability) of $[\text{Ni}(\text{PCH}=\text{NO})_2\text{BF}_2]^+$, $[\mathbf{1}\text{BF}_2]^+$. Most hydrogen atoms were removed for clarity.

1:1 Ni:PNOH/PNO⁻ Complexes. A well-behaved 1:1 complex was prepared by treating PCH=NOH with Ni(C₆F₅)₂(THF)₂. In this reaction, Ni(C₆F₅)₂(THF)₂ is deployed as an anhydrous NiX₂ reagent. The product is [Ni(C₆F₅)(PCH=NO)]₂ (**2**), which was isolated as a yellow solid (Scheme 6). The formation of C₆F₅H byproduct was confirmed by ¹⁹F NMR spectroscopy (Figure S8). Complex **2** was obtained even when PCH=NOH was used in excess.



Scheme 6. Synthesis of [Ni(C₆F₅)(PCH=NO)]₂ (**2**).

X-ray crystallography reveals a centrosymmetric dimer with bridging oximate and terminal C₆F₅ ligands. Nickel is bound by four different donor atoms: C, P, N, O (Figure 6).

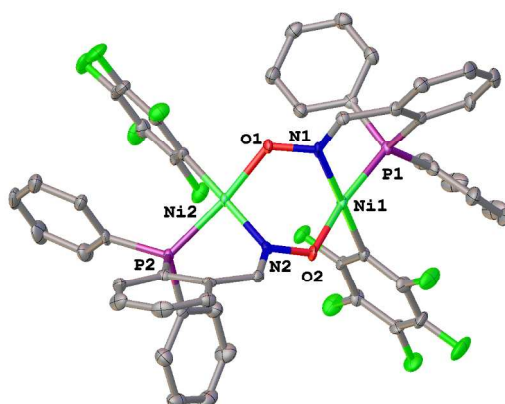
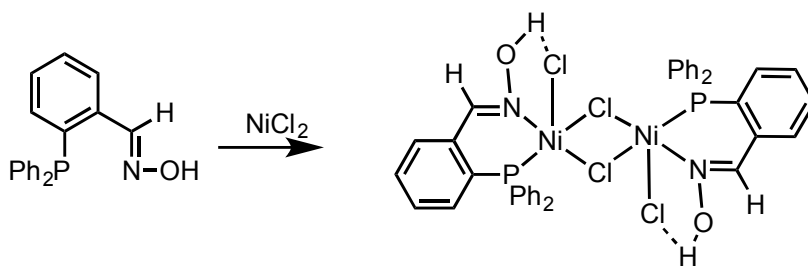


Figure 6. Thermal ellipsoid plot (50% probability) of [Ni(C₆F₅)(PCH=NO)]₂ (**2**). Most hydrogen atoms were removed for clarity.

The Ni centers are square planar ($\tau_4' = 0.0744$ (Ni1); 0.094 (Ni2)) with a deviation from planarity of 0.107 – 0.142 (RMSD/Å). Complex **2** exhibits well-resolved ^{19}F and ^{31}P NMR spectra (Figure S9-S11). The downfield shift of the ^{31}P NMR resonance (δ 32.7) may reflect the electron withdrawing nature of the C_6F_5 substituent.

Combining $\text{PCH}=\text{NOH}$ and equimolar anhydrous NiCl_2 in THF produced yellow $[\text{Ni}(\text{PCH}=\text{NOH})\text{Cl}_2]_2$ (**3**). The phosphine-oxime remains protonated in this complex (Scheme 7).



Scheme 7. Synthesis of $[\text{Ni}(\text{PCH}=\text{NOH})\text{Cl}_2]_2$ (**3**).

This 1:1 complex is a dimeric, with bridging halides as confirmed by X-ray crystallography (Figure 7). This motif is well precedented.¹² The 5-coordinated nickel(II) centers display pseudo trigonal bipyramidal geometry ($\tau = 0.58$). The bond distances of **3** are as follows: Ni-N (~2.07 Å), Ni-P (~2.3 Å), Ni-Cl (~2.3 Å). As seen in $[\mathbf{1H}_2\text{Cl}_2]$, the terminal chloride ligands are hydrogen bonded to the oxime protons ($\text{OH}\cdots\text{Cl} = 2.27$ Å). The bridging chloride ligands, which are expected to be less basic than the terminal chloride ligands, do not interact with the oxime.

10

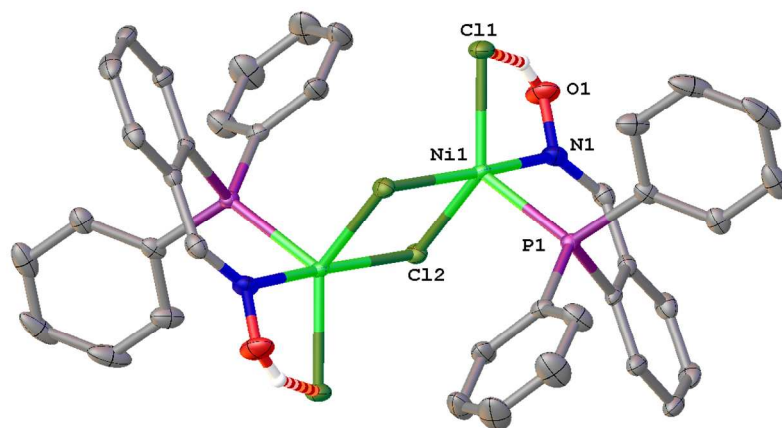


Figure 7. Thermal ellipsoid plot (50 % probability) of [Ni(PCH=NOH)Cl₂]₂ (**3**). Most hydrogen atoms were removed for clarity. The O-H···Cl interaction is denoted by the dashed red line. The unlabeled hetero atoms are related by the symmetry operator (1-x,

Dinickel and Trinickel Complexes. Reflecting the tendency of oximates to serve as bridging ligands,¹³ the most robust complex in the entire series is the orange oxo-bridged cation [Ni₃(PCH=NO)₃O]⁺ ([**4**]⁺). This complex [**4**]⁺ arises from the reaction of PCH=NOH and Ni(BF₄)₂·6H₂O as well as the hydrolysis of [Ni(PCH=NOH)₂](BF₄)₂, Ni(PCH=NOH)Cl₂, [Ni(PCH=NOH)Cl₂]₂, and [Ni(PCH=NO)(C₆F₅)₂] (Figure S12, S13, Scheme S1).

X-ray crystallographic analysis shows that [**4**]⁺ consists of three [Ni(PCH=NO)]⁺ centers linked by bridging oximates (Figure 8). The [Ni₃O] motif is often stabilized by oximate ligands,¹³ but [**4**]⁺ is a rare example of a nickel-oxo-phosphine.¹⁴ The nickel centers in [**4**]⁺ are square planar with short Ni-N (~1.86 Å), Ni-P (~ 2.2 Å), and even Ni-O (~ 1.86 Å) bond distances, consistent with low-spin nature of nickel(II). The ³¹P-NMR spectrum indicates a highly symmetrical structure (Figure S14).

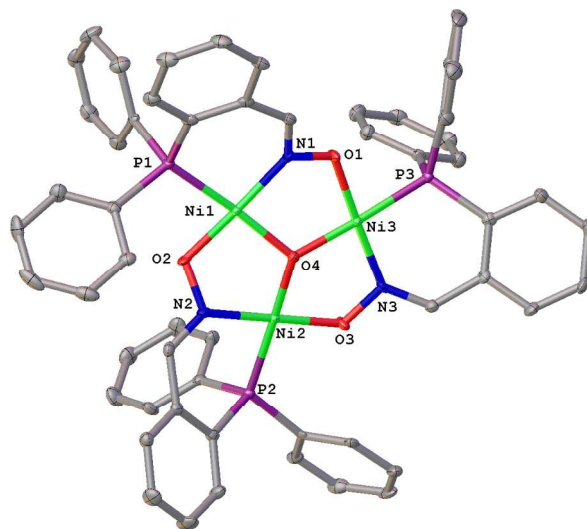


Figure 8. Thermal ellipsoid plot (50 % probability) of $[4]^+$. Most hydrogen atoms were removed for clarity.

The conversion of $[\text{Ni}(\text{MeCN})_6](\text{BF}_4)_2$ and $\text{PCH}=\text{NOH}$ to give $[4]\text{BF}_4$ requires the presence of adventitious water, which forms the oxo ligand. The strong oxophilicity of this reaction is indicated by the observation of $[5](\text{BF}_4)_2$, a byproduct arising from the dehydration of $\text{PCH}=\text{NOH}$. The structure of $[5]^{2+}$ consists of a pair of planar Ni centers supported by three phosphine ligands (Figure 9, Scheme S2, S3). One $\text{PCH}=\text{NOH}$ ligand remains intact, but two have condensed (with loss of water) to generate a diphosphine ligand containing the $\text{C}=\text{N}-\text{O}-\text{C}(\text{R})-\text{N}$ subunit. This motif typically arises via reaction of an oximate and a nitrile.¹⁵ Complex $[5]^{2+}$ retains its structure in dichloromethane solutions, as indicated by the ^{31}P NMR spectrum, which exhibits an AB quartet pattern at δ 23.4 and 25.6, as well as a singlet at δ 21.5 (Figure S15).

12

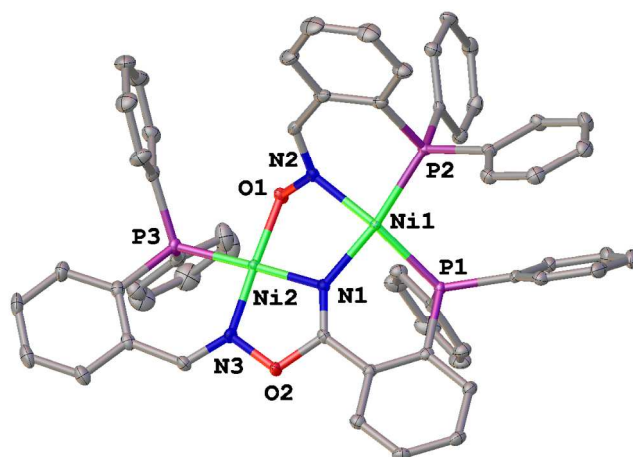


Figure 9. Thermal ellipsoid plot (50 % probability) of [5]²⁺. Most hydrogen atoms were removed for clarity.

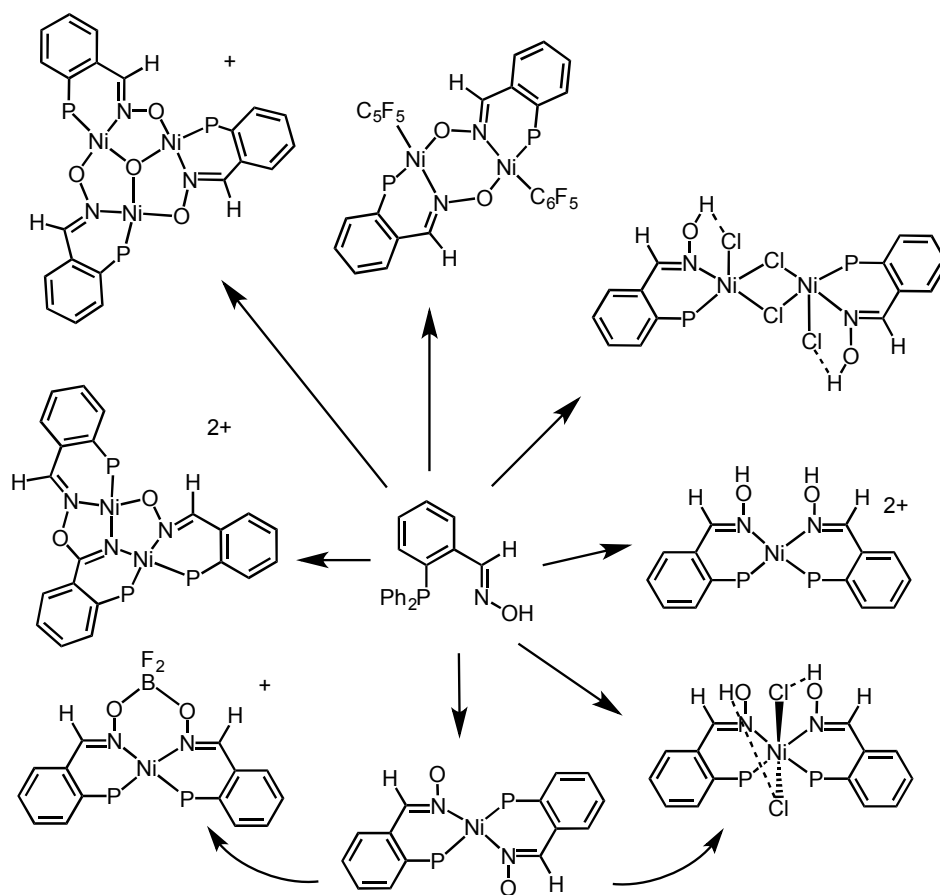


Figure 10. Complexes prepared in this work (Ph groups omitted for clarity).

Conclusions

In summary, a prototypical phosphine-oxime $\text{Ph}_2\text{PC}_6\text{H}_4\text{-2-CH=NOH}$, abbreviated PCH=NOH, affords 2:1 Ni(II) derivatives with rich acid-base behavior. In cases where chloride is a coligand, the oxime engages the anionic coligands by intramolecular hydrogen bonds. Neutral PCH=NOH is labile on Ni(II), which gives rise to a trinickel derivative featuring bridging oximates (Figure 10). The absence of oxime-oximate hydrogen bonds can be attributed to the wide bite angle of the P-N chelate ring. The dioximate derivative is a potential precursor to heterobimetallic derivatives.¹⁶ The dioximate derivative can be enforced by a capping reaction with boron trifluoride. As indicated from the electrochemistry of this capped derivative, these complexes can stabilize lower oxidation state of nickel. These results encourage similar studies on related complexes, where still greater flexibility can be expected with respect to redox states.¹⁷

Experimental

General. Literature procedures were followed for the preparation of $\text{Ph}_2\text{PC}_6\text{H}_4\text{-2-CH=NOH}$,¹⁸ $[\text{Ni}(\text{MeCN})_6](\text{BF}_4)_2$,¹⁹ and $\text{Ni}(\text{C}_6\text{F}_5)_2(\text{dioxane})_2$.²⁰ Other precursors were obtained from commercial sources. Solvents were HPLC grade and were thoroughly dried and deoxygenated on an MBraun solvent purification system and stored over 4 Å molecular sieves. Complexation reactions were performed under an argon or nitrogen atmosphere in a glove box or under Schlenk line. ³¹P, and ¹⁹F NMR spectra were recorded with a Bruker B-500 spectrometer at 25 °C. Chemical shifts are reported in ppm and coupling constants in Hz. ESI mass spectrometric analyses were performed by

the School of Chemical Sciences Mass Spectrometry Laboratory. CHN analyses were performed by the School of Chemical Sciences Microanalysis Laboratory using an Exeter Analytical CE 440 and Perkin Elmer 2440, Series II instruments.

[Ni(PCH=NOH)₂](BF₄)₂ ([1H₂](BF₄)₂). A slurry of [Ni(MeCN)₆](BF₄)₂ (0.239 g, 0.5 mmol) in 5 mL of THF was added to a solution of PCH=NOH (0.305 g, 1 mmol) in 25 mL of THF. After stirring for 2 h at room temperature, the solution was concentrated to a volume of 5 mL. An orange-coloured solid precipitated from the concentrated solution after few hours. X-ray quality crystals were obtained by vapor diffusion of pentane into the CH₂Cl₂ solution of the complex. Yield: 316 mg (75 %). ³¹P NMR (202 MHz, CD₂Cl₂): δ 29.18. Anal. Calcd for C₃₉H₃₄B₂Cl₂F₈N₂NiO₂P₂ [[(1H₂](BF₄)₂).CH₂Cl₂] (found): C, 50.48 (49.83); H, 3.69 (3.37); N, 3.53 (3.2).

[Ni(PCH=NO)₂] ([1]⁰). A solution of Ni(OAc)₂·4H₂O (0.124 g, 0.5 mmol) in 5 mL of MeOH was added to a solution of PCH=NOH (0.305 g, 1 mmol) in 25 mL of CH₂Cl₂. After stirring for 2 h at room temperature, the solution was concentrated to a volume of 5 mL. A red-orange solid precipitated from the concentrated solution after few days. X-ray quality crystals were obtained by two different ways: (i) vapor diffusion of pentane into the CH₂Cl₂ solution of the complex, or (ii) slow evaporation from MeOH/H₂O (9:1) mixture. Yield: 267 mg (80 %). ³¹P NMR (202 MHz, CD₂Cl₂): δ 12.63 (s). Anal. Calcd for C_{39.5}H₃₃Cl₃N₂NiO₂P₂ [(1).1.5CH₂Cl₂] (found): C, 59.70 (59.84); H, 4.19 (4.01); N, 3.53 (3.24).

[Ni(PCH=NOH)₂Cl₂] ([1H₂Cl₂]). A solution of NiCl₂·6H₂O (0.119 g, 0.5 mmol) in 5 mL of MeOH was added to a solution of PCH=NOH (0.305 g, 1 mmol) in 25 mL of CH₂Cl₂. After stirring for 2 h at room temperature, the reaction solution was evaporated

to dryness. Green X-ray quality crystals were obtained by vapor diffusion of Et₂O into the CH₂Cl₂ solution of the complex at -30° C. Yield: 296 mg (80 %). Anal. Calcd for C₄₀H₃₆Cl₆N₂NiO₂P₂ [[(1H₂Cl₂)]₂.2CH₂Cl₂] (found): C, 52.79 (53.02); H, 3.99 (3.5); N, 3.08 (2.91).

[Ni(PCH=NO)₂BF₂]BF₄ [(1)BF₂]BF₄. Boron trifluoride-diethyl etherate BF₃.Et₂O (13 μL, 0.1 mmol) was added dropwise to a solution of [1]⁰ (0.034 g, 0.05 mmol) in 10 mL CH₂Cl₂. Instantly, the color of the solution was changed from dark red to light orange. After stirring for 2 h, the volume of the resulting solution was reduced to 3 mL. Yellow crystalline precipitate was obtained upon slow diffusion of diethyl-ether into the resulting solution at low temp. X-ray quality crystals were obtained upon vapor diffusion of diethylether into CH₂Cl₂/CH₃CN (1:1) solution of the complex at room temp. Yield: 0.028 g (70 %). ³¹P NMR (202 MHz, CH₂Cl₂) δ 26.88 (s); ¹⁹F NMR (470.4 MHz, CH₂Cl₂); δ -153.18 (4F), -157.09 (2F); ESI-MS (positive): [M]⁺ [(1)BF₂]⁺: 715.1204 (100 %). Anal. Calcd for C_{38.5}H₃₁B₂ClF₆N₂NiO₂P₂ [(1)BF₂]BF₄.0.5CH₂Cl₂] (found): C, 54.70 (54.77); H, 3.70 (3.62); N, 3.31 (3.35).

[Ni(C₆F₅)(PCH=NO)]₂ (2). A solution of Ni(C₆F₅)₂(THF)₂ (0.537 g, 1 mmol) in 5 mL THF was added to a solution of PCH=NOH (0.305 g, 1 mmol) in 25 mL of THF. After stirring for 2 h at room temperature, the solution was concentrated to a volume of 5 mL. A yellow colored solid precipitated from the concentrated solution after few hours. X-ray quality crystals were obtained by vapor diffusion of pentane into the CH₂Cl₂ solution of the complex. Yield: 317 mg (70 %). ³¹P NMR (202 MHz, CD₂Cl₂): δ 32.72. ¹⁹F NMR (470.4 MHz, CD₂Cl₂) δ -118.16 (d, 2F); -162.24 (t, 1F); -164.31 (t, 2F) Anal.

Calcd for $C_{51}H_{32}Cl_2F_{10}N_2Ni_2O_2P_2$ [(2).CH₂Cl₂] (found): C, 53.50 (53.33); H, 2.82 (3.62); N, 2.45 (2.25).

[Ni(PCH=NOH)Cl₂]₂ (3). A slurry of NiCl₂ (0.130 g, 1 mmol) in THF (5 mL) was added to a solution of PCH=NOH ligand (0.305 g, 1 mmol) in 20 mL of THF. After stirring for 2 h at room temperature, the volume of the solution was reduced to 5 mL. A yellow coloured solid precipitated from the solution after few days. X-ray quality crystals were obtained by vapor diffusion of pentane into the CH₂Cl₂ solution of the complex. Yield: 370 mg (85 %). Anal. Calcd for $C_{40}H_{36}Cl_4N_2Ni_2O_{2.5}P_2$ [(3).0.5THF] (found): C, 53.04 (53.35); H, 4.01 (3.65); N, 3.09 (2.96).

[Ni₃(PCH=NO)₃O]BF₄ ([4]BF₄). A solution of [Ni(H₂O)₆](BF₄)₂ (0.340 g, 1 mmol) in 5 mL of MeOH was added to a solution of PCH=NOH ligand (0.305 g, 1 mmol) in 25 mL of CH₂Cl₂. After stirring the solution for 2 h at room temperature, the solvent was removed. Slow evaporation of a MeOH/H₂O (9:1) solution of the complex gave orange coloured X-ray quality crystals, which were also used for elemental analysis. Yield: 298 mg (75 %). ³¹P NMR (202 MHz, CD₂Cl₂): δ 22.47. Anal. Calcd for $C_{57}H_{46}BF_4N_3Ni_3O_{4.5}P_3$ [(4]BF₄).0.5 H₂O] (found): C, 57.01 (56.97); H, 3.86 (4.21); N, 3.50 (3.16).

[Ni₂(PCH=NO)(PCH=NO-(C=N)P](BF₄)₂ ([5](BF₄)₂). We obtained the orange colored rearranged product **5**²⁺ as a biproduct along with **4**⁺ when the reaction of PCH=NOH ligand was carried out with [Ni(MeCN)₆](BF₄)₂ in THF in the presence of adventitious water. X-ray quality crystals were obtained by vapor diffusion of pentane into the CH₂Cl₂ solution of the complex at -30 ° C. ³¹P NMR (202 MHz, CD₂Cl₂): δ 25.65 (d, J = 65 Hz); 23.36 (d, J = 66 Hz); 21.46 (s). This compound was not separated from complex [4]BF₄, hence elemental was not taken.

X-ray Crystallographic Determinations. Data for $[\text{Ni}(\text{PCH}=\text{NOH})_2](\text{BF}_4)_2$, $[\text{Ni}(\text{PCH}=\text{NO})_2]$, $[\text{Ni}(\text{PCH}=\text{NO})_2\text{BF}_2]\text{BF}_4$, $[\text{Ni}(\text{C}_6\text{F}_5)(\text{PCH}=\text{NO})]_2$, $[\text{Ni}(\text{PCH}=\text{NOH})\text{Cl}_2]_2$, $[\text{Ni}_3(\text{PCH}=\text{NO})_3\text{O}]\text{BF}_4$, and $[\text{Ni}_2(\text{PCH}=\text{NO})(\text{PCH}=\text{NO}-(\text{C}=\text{N})\text{P})(\text{BF}_4)_2]$ were collected on a Bruker D8 Venture diffractometer equipped with a four-circle kappa diffractometer and Photon 100 detector. An I μ s microfocus Mo source ($\lambda = 0.71073 \text{ \AA}$) coupled with a multi-layer mirror monochromator supplied the incident beam. Data for $[\text{Ni}(\text{PCH}=\text{NOH})_2\text{Cl}_2]$ was collected on a Bruker Kappa four-circle diffractometer equipped with an APEXII CCD detector. A fine-focus sealed tube Mo source ($\lambda = 0.71073 \text{ \AA}$) coupled with a graphite monochromator supplied the incident beam. The samples were mounted on a 0.3 mm nylon loop with the minimal amount of Paratone-N oil. Data were collected as a series of φ and/or ω scans. Data were collected at 100K and integrated and filtered for statistical outliers using SAINT²¹, then corrected for absorption by either semi-empirical methods ($[\mathbf{1H}_2](\text{BF}_4)_2$, $[\mathbf{(1)BF}_2]\text{BF}_4$, **(2)**, **(3)**, **[4]BF}_4, and **[5](BF}_4)_2**) or integration ($[\mathbf{1}]^0$ and $[\mathbf{1H}_2\text{Cl}_2]$) using SADABS²². The structures were phased using direct methods (SHELXS)²³ for $[\mathbf{1H}_2](\text{BF}_4)_2$, $[\mathbf{1H}_2\text{Cl}_2]$, and **(2)** or intrinsic phasing methods (SHELXT)²⁴ for $[\mathbf{1}]^0$, $[\mathbf{(1)BF}_2]\text{BF}_4$, **(3)**, **[4]BF}_4, and **[5](BF}_4)_2** and then refined with the full-matrix least-squares program SHELXL.²³****

References

1. (a) R. Bigler, E. Otth and A. Mezzetti, *Organometal.*, 2014, **33**, 4086; (b) H. P. Lane, M. Watkinson, N. Bricklebank, C. A. McAuliffe and R. G. Pritchard, *Inorg. Chim. Acta*, 1995, **232**, 145; (c) M. Ranocchiari and A. Mezzetti, *Organometal.*, 2009, **28**, 1286.
2. (a) K. L. Bray, C. P. Butts, G. C. Lloyd-Jones and M. Murray, *J. Chem. Soc., Dalton Trans.*, 1998, 1421; (b) A. Kermagoret, F. Tomicki and P. Braunstein, *Dalton Trans.*, 2008, 2945; (c) P. Chavez, I. G. Rios, A. Kermagoret, R. Pattacini, A. Meli, C. Bianchini, G. Giambastiani and P. Braunstein, *Organometal.*, 2009, **28**, 1776.

3. A. D. Schmidt, Y. Sun and W. R. Thiel, *Z. Anorg. Allg. Chem.*, 2015, **641**, 2093.
4. M. O'Reilly, R. Pattacini and P. Braunstein, *Dalton Trans.*, 2009, 6092.
5. B. Biswas, U. Pieper, T. Weyhermuller and P. Chaudhuri, *Inorg. Chem.*, 2009, **48**, 6781.
6. (a) P-A. Jacques, V. Artero, J. Pécaut and M. Fontecave, *Proc. Natl. Acad. Sci.*, 2009, **106**, 20627; (b) S. Cherdo, S. E. Ghachtouli, M. Sircoglou, F. Brisset, M. Oriob and A. Aukauloo, *Chem. Commun.*, 2014, **50**, 13514.
7. (a) C. Tsay and J. Y. Yang, *J. Am. Chem. Soc.*, 2016, **138**, 14174; (b) A. D. Wilson, R. K. Shoemaker, A. Miedaner, J. T. Muckerman, D. L. DuBois and M. R. DuBois, *Proc. Natl. Acad. Sci.*, 2007, **104**, 6951; (c) L. Gan, T. L. Groy, P. Tarakeshwar, S. K. S. Mazinani, J. Shearer, V. Mujica and A. K. Jones, *J. Am. Chem. Soc.*, 2015, **137**, 1109.
8. (a) L. Menéndez-Rodríguez, E. Tomás-Mendivil, J. Francos, C. Nájera, P. Crochet and V. Cadierno, *Catal. Sci. Technol.*, 2015, **5**, 3754; (b) J. Francos, L. Menendez-Rodriguez, E. Tomas-Mendivil, P. Crochet and V. Cadierno, *RSC Adv.*, 2016, **6**, 39044; (c) K. Park, P. O. Lagaditis, A. J. Lough and R. H. Morris, *Inorg. Chem.*, 2013, **52**, 5448.
9. W. Keim and R. P. Schulz, *J. Molec. Catal.*, 1994, **92**, 21.
10. (a) S. Zhang, R. Pattacini, S. Jiea and P. Braunstein, *Dalton Trans.*, 2012, **41**, 379; (b) M. Polamo and T. V. Laine, *Z. Kristallogr.*, 2007, **222**, 13.
11. T. Yoshioka, K. Matsushima, G. Hihara and H. Miyamae, *Anal. Sci.: X-ray Struct. Anal.*, 2006, **22**, x205.
12. (a) A. Kermagoret and P. Braunstein, *Organometal.*, 2008, **27**, 88; (b) W-H. Sun, Z. Li, H. Hu, B. Wu, H. Yang, N. Zhu, X. Leng and H. Wang, *New J. Chem.*, 2002, **26**, 1474; (c) F. Speiser, P. Braunstein, L. Saussine and R. Welter, *Inorg. Chem.*, 2004, **43**, 1649.
13. (a) A. Audhya, M. Maity, K. Bhattacharya, R. Clerac and M. Chaudhury, *Inorg. Chem.*, 2010, **49**, 9026; (b) L. K. Das, A. Biswas, J. S. Kinyon, N. S. Dalal, H. Zhou and A. Ghosh, *Inorg. Chem.*, 2013, **52**, 11744; (c) A. Audhya, K. Bhattacharya, M. Maity and M. Chaudhury, *Inorg. Chem.*, 2010, **49**, 5009.
14. M. M. Shoshani, R. Beck, X. Wang, M. J. McLaughlin and S. A. Johnson, *Inorg. Chem.*, 2018, **57**, 2438.
15. (a) V. V. Pavlishchuk, S. V. Kolotilov, A. W. Addison, M. J. Prushan, R. J. Butcher and L. K. Thompson, *Inorg. Chem.*, 1999, **38**, 1759; (b) V. V. Pavlishchuk, S. V. Kolotilov, A. W. Addison, M. J. Prushan, R. J. Butcher and L. K. Thompson, *Chem. Commun.*, 2002, 468; (c) O. Das, N. N. Adarsh, A. Paul and T. K. Paine, *Inorg. Chem.*, 2010, **49**, 541; (d) E. V. Andrusenko, E. V. Kabin, A. S. Novikov, N. A. Bokach, G. L. Starova, A. A. Zolotarev and V. Y. Kukushkin, *Eur. J. Inorg. Chem.*, 2015, 4894; (e) M. N. Kopylovich, V. Y. Kukushkin, M. Haukka, K. V. Luzyanin and A. J. L. Pombeiro, *J. Am. Chem. Soc.*, 2004, **126**, 15040.
16. D. A. Henckel, Y. F. Lin, T. M. McCormick, W. Kaminsky and B. M. Cossairt, *Dalton Trans.*, 2016, **45**, 10068.
17. (a) D. Basu, S. Mazumder, J. Niklas, H. Baydoun, D. Wanniarachchi, X. Shi, R. Staples, O. Poluektov, H. B. Schlegel and C. N. Verani, *Chem. Sci.*, 2016, **7**, 3264; (b) A. Bhattacharjee, E. S. Andreiadis, M. Chavarot-Kerlidou, M. Fontecave, M. J. Field and V. Artero, *Chem. Eur. J.*, 2013, **19**, 15166.

18. L. Xu, D. Zhu, F. Wu, R. Wang and B. Wan, *Tetrahedron*, 2005, **61**, 6553.
19. R. A. Heintz, J. A. Smith, P. S. Szalay, A. Weisgerber and K. R. Dunbar, *Inorg. Synth.*, 2002, **33**, 75.
20. (a) A. Arcas and P. Royo, *Inorg. Chim. Acta*, 1978, **30**, 205; (b) A. Arcas and P. Royo, *Inorg. Chim. Acta*, 1978, **31**, 97; (c) J. Fornies, A. Martin, L. F. Martin, B. Menjon, H. A. Kalamarides, L. F. Rhodes, C. S. Day and V. W. Day, *Chem. Eur. J.*, 2002, **8**, 4925.
21. Bruker (2014). SAINT, SHELXTL, XCIF, XPREP. Bruker AXS, Inc., Madison, Wisconsin, USA.
22. L. Krause, R. Herbst-Irmer, G. M. Sheldrick and D. Stalke, *J. Appl. Cryst.*, 2015, **48**, 3.
23. G. M. Sheldrick, *Acta Cryst.*, 2015, **C71**, 3.
24. G. M. Sheldrick, *Acta Cryst.*, 2015, **A71**, 3.

